International Journal of Power and Energy Systems, Vol. 46, No. 10, 2026
An Open Access Paper

A FAULT LOCALIZATION METHOD FOR MULTI-BRANCH OVERHEAD LINES BASED ON CLOUD-EDGE COLLABORATION

Ziming Zhu,* Xiaoyong Yu,* Ke Zhou,* Tanghua Wu**

Abstract

Aiming at the problems of insufficient fault localization accuracy of multi-branch overhead lines and the limited real-time performance of existing centralized architectures, this study proposes a hierarchical fault localization method based on cloud-edge collaboration. By integrating the high-frequency signal acquisition capabilities at the edge with the in-depth data analysis advantages of the cloud, this method achieves efficient processing of fault signals and fusion of multi-source data. A fault distance matrix is established based on the principle of dual-terminal traveling wave ranging, and a fault determination matrix is generated in combination with a defined structural distance matrix. The algorithm's anti-interference capability is enhanced through differential operations and correction margins. Simulation experiments demonstrate that the proposed method achieves localization errors of less than 20 meters across various fault scenarios. Quantitative comparison with conventional methods confirms a significant enhancement in localization performance, with error reduction ranging from approximately 74.4% to 91.4%. Compared with traditional single-ended methods and artificial intelligence algorithms, it demonstrates significant improvements in adaptability to complex network topologies, dynamic response efficiency, and fault tolerance, providing a new approach for intelligent fault localization in distribution networks.

Key Words

Multi-branch overhead lines; cloud-edge collaboration; fault localization; traveling-wave-based ranging

* Electric Power Research Institute of Guangxi Power Grid Co., Ltd, Nanning, China; e-mail: zhuyali03@126.com, yuhouwu09@sina.com, zhouby@keylabtory.com
** Qinzhou New District Power Supply Bureau of Guangxi Power Grid Co., Ltd; e-mail: wu202167@163.com
Corresponding Author: Tanghua Wu

Recommended by: Bishwajit Dey
(DOI: 10.2316/J.2026.203-0633)

1. Introduction

Distribution networks are becoming more complex. Distributed generation and diverse loads increase operational uncertainty. In multi-branch overhead lines, dispersed topologies and tight node coupling make traditional fault localization vulnerable to signal attenuation, measurement errors, and synchronization offsets, reducing accuracy and real-time performance. Centralized diagnosis that relies on central servers cannot meet the timeliness required as edge computing capabilities grow. Long, branch-disturbed signal paths in complex distribution networks further impede accurate and rapid fault localization [1]-[2].

The complex structure and numerous branches of distribution networks extend fault signal paths and cause disturbances, hindering accurate fault identification and rapid localization [3]-[5]. Currently, fault localization techniques mainly include fault analysis, artificial intelligence algorithms, and traveling wave methods. Fault analysis is divided into single-ended and double-ended methods based on data collection location. Single-ended methods use node impedance matrices with equivalent models. They are low-cost but sensitive to noise and topology, often producing false fault points. Conte et al. [6] used a single-ended impedance method with PMU data, but extra screening for false points raises computational cost and limits adaptability to dynamic distributed energy. Dual-ended methods are further classified based on whether synchronized data are needed. Chandran et al. [7] proposed a phase-comparison scheme using pre- and post-fault phase differences, but it requires synchronized devices, hindering engineering applications. Arsoniadis and Nikolaidis [8] proposed a non-synchronized dual-ended method modifying the impedance matrix, but dependence on measurement points and complex operations restricts feeder automation use. Zhao et al. [9] located fault sections using zero-sequence current centroid frequency differences, but accuracy drops when the grounding phase angle is small. To address the sensitivity of fault analysis to parameter disturbances, AI methods attract attention for strong fault tolerance and low model dependence. Approaches based on genetic algorithms [10], expert systems [11], and ant colony

algorithms [12] demonstrate robust fault tolerance in complex systems. However, they depend on accurate topology and full coverage of fault scenarios. With growing network complexity and fault diversity, algorithmic load has significantly increased, limiting response speed, flexibility, and engineering adaptability [13]-[14].

The traveling wave method is widely applied in transmission grids as it is insensitive to fault types and transition resistances [15]-[17]. However, short lines and complex structures in distribution networks hinder their direct application. Zhao et al. [18] proposed locating single-phase ground faults using traveling wave time–frequency characteristics, but its dependence on wavefront identification and high-sampling-rate equipment limits adoption. The single-ended method [19] is simple, yet branch lines cause multiple reflections and refractions, leading to signal superposition and interference that complicate wavefront identification. Zhang et al. [20] introduced a single-ended time-domain method that reduces branch effects without remote data, but it is highly sensitive to zero-sequence wave velocity and lacks robustness. The dual-ended method [21]-[22] captures initial signals at both line ends, avoiding complex reflection analysis and providing a fast response with high accuracy. Cheng et al. [23] developed a time-matrix approach using multi-ended synchronized data, but its application remains constrained in complex distribution networks.

To address the aforementioned issues, this paper proposes a fault localization method for multi-branch overhead lines based on cloud–edge collaboration. By integrating high-frequency signal acquisition at the edge with deep cloud-based analysis, the method enables efficient fault signal processing and multi-source data fusion. Fault distance matrices [24] are constructed based on the dual terminal traveling wave ranging principle and combined with structural distance matrices to generate fault determination matrices, improving anti-interference capability and localization accuracy. Simulation results show that the proposed method achieves localization errors below 20 m under various fault scenarios, reducing errors by 74.4%–91.4% compared with traditional approaches, demonstrating strong engineering applicability and adaptability to complex topologies.

The structure of this paper is arranged as follows: Section 2 analyzes traveling wave propagation in Y-type topologies, derives distance matrix expressions for different fault locations, and reveals the correlation between matrix elements and fault positions. Section 3 builds the cloud-edge framework, generates the fault determination matrix by differencing structural and fault distance matrices, and localizes the fault based on matrix characteristics. Section 4 presents simulations showing that under various fault scenarios, localization errors remain within 20 meters. Finally, the paper concludes with a summary and discussion of future research directions.

2. Fault Traveling Wave Transmission Path

Fig. 1 shows the Y-type topology of overhead distribution lines with node T as the junction of three branches. Traveling wave acquisition devices are placed at each branch terminal. Before any fault, a traveling wave is injected at M_1 and propagates toward M_2 and M_3, with propagation distances as follows:

$$\begin{cases} d_{M2M1} = d_{M2T} + d_{M1T} \\ d_{M3M1} = d_{M3T} + d_{M1T} \end{cases} \tag{1}$$

Where d_{M1T}, d_{M2T} and d_{M3T} denote the distances from terminals M_1, M_2, and M_3 to the junction node T, respectively.

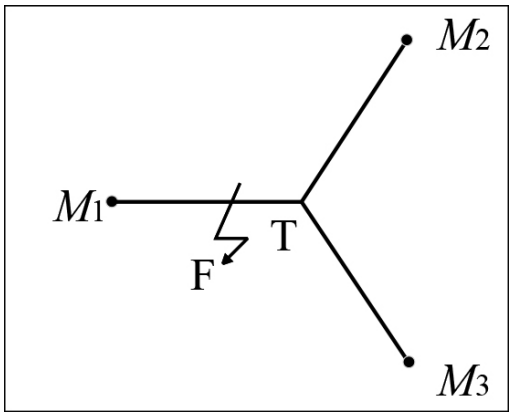

Figure 1. Y-shaped Topology of Overhead Distribution Lines

By rearranging (1), the following expression is obtained:

$$\begin{cases} \Delta d_{M1M2} = -d_{M1T} - d_{M2T} \\ \Delta d_{M1M3} = -d_{M1T} - d_{M3T} \\ \Delta d_{M2M3} = d_{M2T} - d_{M3T} \end{cases} \tag{2}$$

When a fault occurs at point F on the M_1T section of the line, the distances from the fault point to each terminal of the network are as follows:

$$\begin{cases} d_{M1F} = d_{M1T} - d_{FT} \\ d_{M2F} = d_{M2T} + d_{FT} \\ d_{M3F} = d_{M3T} + d_{FT} \end{cases} \tag{3}$$

where d_{FT} denotes the distance between the junction node T and the fault point F.

By pairwise subtraction of (3), the following expression is obtained:

$$\begin{cases} \Delta d_{M1M2F} = d_{M1T} - d_{M2T} - 2d_{FT} \\ \Delta d_{M1M3F} = d_{M1T} - d_{M3T} - 2d_{FT} \\ \Delta d_{M2M3F} = d_{M2T} - d_{M3T} \end{cases} \tag{4}$$

Taking the terminal nodes of each feeder as reference points, the distance matrix d is constructed. The mathematical expression is as follows:

$$d = \begin{bmatrix} 0 & \Delta d_{M2M1F} - \Delta d_{M2M1} & \Delta d_{M3M1F} - \Delta d_{M3M1} \\ \Delta d_{M1M2F} - \Delta d_{M1M2} & 0 & \Delta d_{M3M2F} - \Delta d_{M3M2} \\ \Delta d_{M1M3F} - \Delta d_{M1M3} & \Delta d_{M2M3F} - \Delta d_{M2M3} & 0 \end{bmatrix} \tag{5}$$

By substituting (2) and (4) into (5), the relative position between the injection point and fault location F is analyzed through three typical cases.

(1) The injection point M1 and the fault location F are on the same feeder section and coincide.

$$d = \begin{bmatrix} 0 & 0 & 0 \\ 0 & 0 & 0 \\ 0 & 0 & 0 \end{bmatrix} \tag{6}$$

(2) The injection point M_1 and the fault location F are on the same feeder branch and coincide at the same point.

$$d = \begin{bmatrix} 0 & 2d_{FT} - 2d_{M1T} & 2d_{FT} - 2d_{M1T} \\ 2d_{M1T} - 2d_{FT} & 0 & 0 \\ 2d_{M1T} - 2d_{FT} & 0 & 0 \end{bmatrix} \tag{7}$$

(3) The injection point M1 and the fault location F are situated on different branches.

$$d = \begin{bmatrix} 0 & -2(d_{M1T} + d_{FT}) & -2d_{M1T} \\ 2(d_{M1T} + d_{FT}) & 0 & 2d_{FT} \\ 2d_{M1T} & -2d_{FT} & 0 \end{bmatrix} \tag{8}$$

Equations (6)-(8) show that each element of matrix d depends on the relative positions of fault localization F and injection point M_1; ideally, when F coincides with M_1, all elements approach zero.

3. Fault Localization Method Based on Cloud-Edge Collaboration

3.1 Cloud-Edge Collaborative Scheme

This paper proposes a cloud-edge collaborative architecture for enhancing the real-time performance and robustness of fault localization in multi-branch overhead distribution lines, as shown in Fig. 2. It combines rapid edge response with deep cloud analysis to enable fault localization in multi-branch overhead lines [25] [26]. Traveling wave-based devices are installed at key nodes (e.g., M_1–M_6) to capture high-frequency signals and extract fault features in real time. Collected data is sent from the edge to the control center via a high-speed, reliable network. The control center immediately performs preliminary processing upon reception. A structural distance matrix **D** is then constructed to reflect the network's topological distances. Simultaneously, a fault distance matrix **d** is calculated using the double-ended traveling wave principle. The difference between matrices **D** and **d** is then computed to derive the fault judgment matrix δ, which is further corrected to enhance localization accuracy. The master station then localizes the fault section, first checking the reference node, and if not, determining whether the fault is within a branch or along the line between nodes. After identifying the fault section, a dedicated algorithm performs precise fault localization. Leveraging precise edge data and deep cloud analysis, the cloud-edge system enables accurate fault diagnosis and localization in the distribution network.

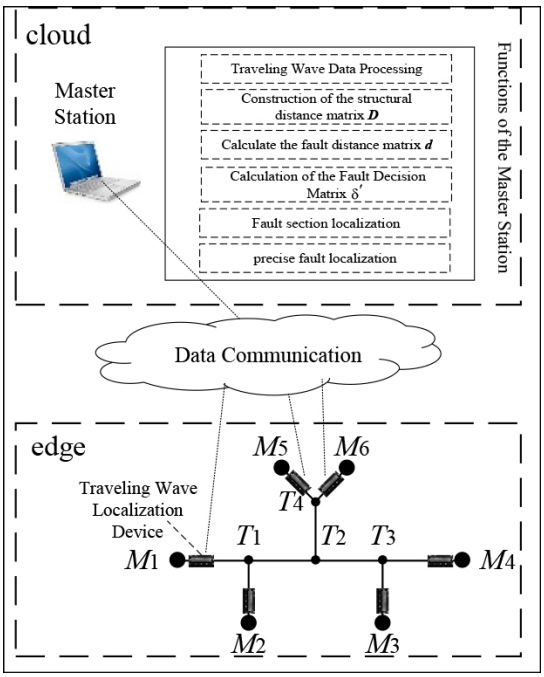

Figure 2. Cloud-Edge Collaborative System Framework

3.2 Construction of the Fault Diagnosis Matrix

In overhead transmission lines, each main feeder typically comprises multiple branch nodes, and the branch lines themselves may further extend into sub-branch nodes. As illustrated in Fig. 3, lines M_1–M_6 represent the end lines of each branch. Nodes T_1, T_2, and T_3 connect the branches to the main feeder, while T_4 is a sub-branch node linking M_5 at T_2 to M_6 at T_4. The main feeder from M_1 to M_4 forms a special feeder structure composed of segments M_1T_1, T_1T_2, T_2T_3, and M_4T_3.

In the absence of faults, line terminals are set as reference ends, and their branch nodes as reference nodes. For example, if M_1 or M_2 are reference terminals, the associated reference node is T_1; if M_5 or M_6 are reference terminals, the corresponding reference nodes are T_2 and T_4. The difference between the reference branch M_i and

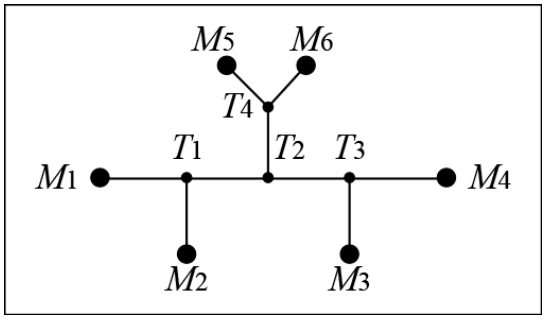

Figure 3. Multi-branch Overhead Line Topology

the branch M_j at the opposite terminal is given by:

$$D_{MiMj} = D_{MiTk} - D_{MjTk} \tag{9}$$

In the formula, T_k denotes the reference node corresponding to the reference terminal M_i. D_{MiTk} represents the distance from node M_i to the reference node T_k. D_{MjTk} represents the distance from node M_j to the reference node T_k. When the topology of the overhead line is determined, a structural distance matrix of size $m \times n$ can be established, where m is the total number of nodes, and n is the number of feeder branches equipped with traveling wave acquisition devices. The structural distance matrix is defined as:

$$D = \begin{bmatrix} 0 & D_{M2M1} & D_{M3M1} & \cdots & D_{MnM1} \\ D_{M1M2} & 0 & D_{M3M2} & \cdots & D_{MnM2} \\ D_{M1M3} & D_{M2M3} & 0 & \cdots & D_{MnM3} \\ \vdots & \vdots & \vdots & \ddots & \vdots \\ D_{M1Mn} & D_{M2Mn} & D_{M3Mn} & \cdots & 0 \end{bmatrix} \tag{10}$$

After a fault occurs, according to the principle of double-ended traveling wave fault localization, the difference in distance from the end of each feeder branch to the fault point can be determined.

$$d_{MiMj} = d_{MiF} - d_{MjF} \tag{11}$$

In the formula, d_{MiF} and d_{MjF} denote the distances from nodes M_i and M_j to the fault localization, respectively. Therefore, based on the topology of the overhead line with m nodes and n branches, the fault distance matrix can be constructed as follows:

$$d = \begin{bmatrix} 0 & d_{M2M1} & d_{M3M1} & \cdots & d_{MnM1} \\ d_{M1M2} & 0 & d_{M3M2} & \cdots & d_{MnM2} \\ d_{M1M3} & d_{M2M3} & 0 & \cdots & d_{MnM3} \\ \vdots & \vdots & \vdots & \ddots & \vdots \\ d_{M1Mn} & d_{M2Mn} & d_{M3Mn} & \cdots & 0 \end{bmatrix} \tag{12}$$

The Fault detection matrix δ can be derived by simultaneously solving (10) and (12):

$$\delta = d - D \tag{13}$$

3.3 Fault Detection Principle

This paper analyzes faults at key nodes and branches in multi-branch overhead lines, using fault traveling wave propagation and the determination matrix, to establish criteria for fault branch localization.

(1) Fault Identification at Reference Nodes
In a multi-branch overhead line, a fault at a reference node falls into two cases: first, the node is a shared connection point for multiple branches; second, the node serves as the reference node for only a single branch. For example, in Fig. 3, a fault at node T_1, common to branches M_1T_1 and M_2T_1, the fault detection matrix constructed based on the matrix difference method indicates that all elements in the corresponding column will be zero, i.e.,

$$\begin{cases} \delta(,1) = [0]_n^T \\ \delta(,2) = [0]_n^T \end{cases} \tag{14}$$

In the formula, $\delta(,1)$ and $\delta(,2)$ denote the elements of the first and second columns of matrix δ, respectively. By analogy, when the fault is located at a node connected by only one branch (e.g., node T_2 on feeder M_5T_2), the corresponding column likewise exhibits the characteristic distribution of zero elements.

$$\delta(,5) = [0]_n^T \tag{15}$$

Based on this, it can be concluded that if all elements in a certain column of the decision matrix are zero, the fault occurs at the branch reference node corresponding to that column, namely:

$$\delta(,i) = [0]_n^T, i = 1, 2, \cdots, n \tag{16}$$

(2) Branch Internal Fault Identification Criterion
If a fault occurs on a specific feeder branch (e.g., branch M_iT_k), it is reflected in the fault matrix such that all elements in the i-th column are less than or equal to zero, while all elements in the i-th row are greater than or equal to zero. Formally, this can be expressed as:

$$\begin{cases} max(\delta(,i)) \le 0 \\ min(\delta(i,)) \ge 0 \end{cases}, i = 1, 2, \cdots, n \tag{17}$$

Such a characteristic suggests that the fault lies on the path between branch M_i and its corresponding reference node T_k, which can be utilized as a diagnostic criterion for locating the faulted branch.

(3) Multi-node Line Fault Identification
In the case where a fault occurs on the line segment between two adjacent T-nodes, the simultaneous solution of (10) to (13) reveals that the fault identification matrix possesses the following properties.

$$\delta(,i) \cdot \delta(,j) = 0 i, j = 1, 2, \cdots, n \tag{18}$$

In this expression, $\delta(,i)$ and $\delta(,k)$ represent the entries of the i-th and j-th columns of matrix c, respectively.

If the dot product of column M_i and column M_j in the coefficient matrix δ is zero, it indicates that the fault point is located between the reference nodes associated with M_i and M_j.

Considering possible measurement errors, noise, or synchronization deviations that may slightly shift elements expected to be zero in the judgment matrix, a correction margin is introduced to enhance algorithm adaptability and fault tolerance. Specifically, any matrix element whose value falls within the interval $[-\varepsilon, +\varepsilon]$ is treated as zero. In this study, the correction margin is set to $\pm 50m$, i.e.,

$$\delta_{ij} = \begin{cases} 0 & \text{if } |\delta_{ij}| \leq \varepsilon \\ \delta_{ij}, & \text{otherwise} \end{cases} \tag{19}$$

3.4 Fault Localization Methodology

After determining the faulty branch, the fault judgment matrix can be used to accurately locate the fault point with the terminal node M_i corresponding to that branch in the fault decision matrix. To enhance the accuracy of fault localization, the arithmetic mean D_N of the elements in the column associated with M_i is first calculated. Subsequently, the distance from terminal node M_i to its associated reference node T_k, denoted as D_{MiTk}, is added to half of the mean value $\frac{D_N}{2}$. This sum yields the estimated distance from node M_i to the actual fault point.

$$dM_i = D_{MiTk} + \frac{D_N}{2} \tag{20}$$

The specific workflow of the fault localization method is presented in Fig. 4.

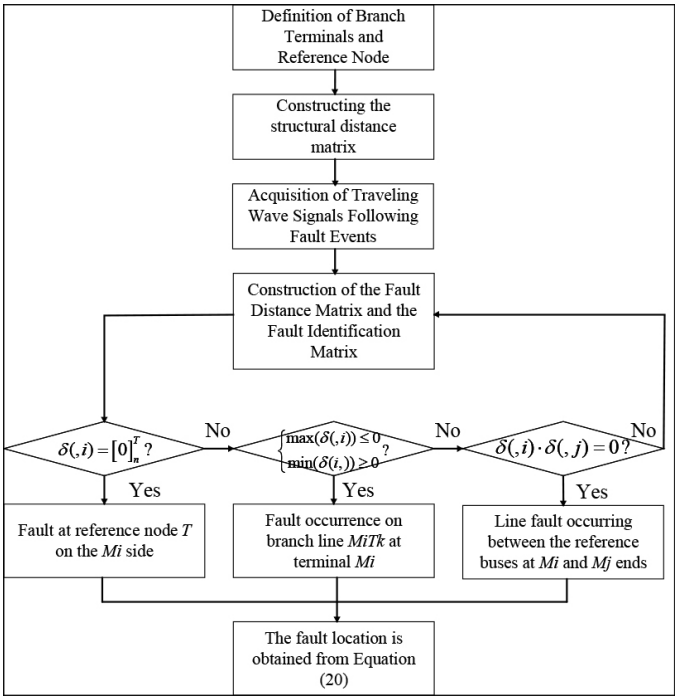

Figure 4. Fault Localization Process Flowchart

4. Simulation-Based Validation

Build a multi-branch overhead line model in the ATP/EMTP software. The model diagram is shown in Fig. 5. The terminal nodes of each branch are designated as $M_1, M_2, M_3, M_4, M_5, M_6$ and M_7, respectively. The length of all line segments is expressed in kilometers. Traveling wave signal acquisition devices are configured at the end of all lines. For the unity of simulation conditions, all overhead lines are set to have the same physical parameters.

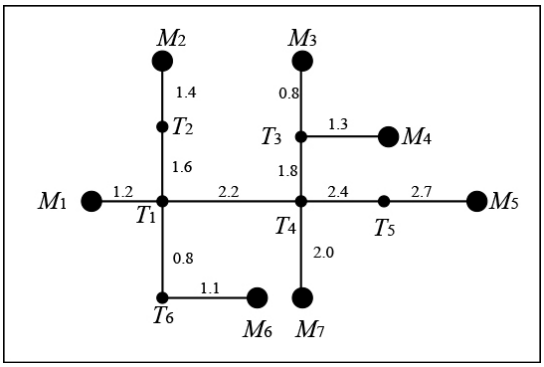

Figure 5. Multi-branch Overhead Line Model Diagram

The fault signal sampling frequency was set at 10 MHz. The collected traveling wave signals are processed using a cubic B-spline wavelet transform to extract the time characteristics of the first arrival of the zero-mode traveling wave components at each monitoring point. Through simulation calculations, the average propagation speed of fault traveling waves in overhead lines is approximately $2.975 \times 10^5 km/s$, with negligible variations in wave speed across different branches. Prior to the occurrence of a fault, based on the known topology and branch parameters, the structural distance matrix can be obtained as follows:

$$D = \begin{bmatrix} 0 & -1.2 & -4.4 & -3.9 & -3.1 & -0.9 & -1.4 \\ -1.8 & 0 & -6 & -5.7 & -4.9 & -2.7 & -3.2 \\ -3.6 & -5 & 0 & 0.5 & -2.3 & -4.5 & -0.6 \\ -4.1 & -5.5 & -0.5 & 0 & -2.8 & -5 & -1.1 \\ -6.1 & -7.5 & -6.1 & -5.6 & 0 & -7 & -3.1 \\ -0.7 & -2.1 & -5.1 & -4.6 & -3.8 & 0 & -2.1 \\ -3 & -4.4 & -3 & -2.5 & -1.7 & -3.9 & 0 \end{bmatrix}$$

4.1 Fault at the Reference Node T

Various typical fault scenarios are set at different T-junction nodes along the feeder. For the case of a phase-A ground fault occurring at node T_3. the fault traveling wave signals at both ends of the line are collected. The acquired signals are analyzed and processed using wavelet transform methods to extract the time information of the initial fault traveling wave arriving at each end. The detection results are shown in Table 1.

By integrating the dual-end traveling wave fault localizatCombined with the double-terminal traveling wave distance measurement algorithm and Formula (12), the fault distance matrix d can be further calculated. The fault

Table 1
Fault Traveling Wave Arrival Time at the Detection Terminal

Detection Terminal	line-mode time / μ s	Detection Terminal	line-mode time / μ s
M_1	4.1	M_4	17.2
M_2	7.4	M_5	22.2
M_3	16.1	M_6	24.5

Table 2
Fault Localization Outcomes under Node Fault Conditions

Fault Location	Types of Faults	transition resistance /Ω	reference terminal	Fault Distance /km	Fault localization distance /km	fault localization error /m
T_1	DLG	100	M_1	1.2	1.187	13
T_2	LL	400	M_2	1.4	1.390	10
T_3	SLG	600	M_3	0.8	0.792	8
	SLG	200	M_4	1.3	1.296	4
T_4	3LG	1000	M_7	2	1.991	9
T_5	OCF	300	M_5	2.7	2.692	8
T_6	LL	800	M_6	1.1	1.088	12

distance matrix d and the structural distance matrix D are subjected to difference calculation to obtain the fault determination matrix δ, and correction processing is performed on it according to the correction principle to obtain the corrected fault determination matrix δ'.

$$\delta' = \begin{bmatrix} 0 & 1.364 & 0 & 0 & 3.126 & 4.164 & 4.135 \\ 6.123 & 0 & 0 & 0 & 5.156 & 7.941 & 5.278 \\ 5.364 & 3.178 & 0 & 0 & 4.356 & 0 & 4.365 \\ 4.258 & 0 & 0 & 0 & 5.315 & 4.268 & 4.687 \\ 4.729 & 2.137 & 0 & 0 & 0 & 8.374 & 6.148 \\ 6.594 & 3.489 & 0 & 0 & 4.278 & 0 & 7.195 \\ 3.478 & 4.513 & 0 & 0 & 6.231 & 4.381 & 0 \end{bmatrix}$$

From the corrected judgment matrix, it can be seen that the elements in the 3rd column and the 4th column are all zero, satisfying $\delta(,3) = [0]_n^T, \delta(,4) = [0]_n^T$. Moreover, since the M_3 terminal and the M_4 terminal share the reference node T_3. It can be determined that the fault occurs in the common branch section T_3 of M_3 and M_4.

According to (20), the distances from the fault localization to the M_3 and M_4 terminals are derived as:

$$\begin{cases} dM_3 = 0.8 - 0.008 = 0.792 \text{ km} \\ dM_4 = 1.3 - 0.004 = 1.296 \text{ km} \end{cases}$$

From this, the estimated distances from the fault location to the ends of line M_3 and M_4 are calculated as $0.792km$ and $1.296km$, respectively. Compared with the actual fault position, the absolute errors are $8m$ and $4m$, respectively. Similarly, the fault localization results for other nodes under different fault conditions are summarized in Table 2.

4.2 Faults on Branch Lines

Simulation of different fault types at various branches in a multi-branch overhead line network. When a three-phase ground fault occurs at $0.7km$ from the M_2 terminal on branch M_2T_2, the fault detection correction matrix is obtained as follows:

$$\delta' = \begin{bmatrix} 0 & -1.435 & 3.158 & 5.368 & 7.266 & 3.144 & 4.364 \\ 9.257 & 0 & 1.427 & 4.364 & 4.341 & 3.148 & 6.258 \\ 4.587 & -1.487 & 0 & 5.149 & 6.214 & 6.254 & 6.145 \\ 5.678 & -1.462 & 6.254 & 0 & 7.268 & 4.365 & 6.249 \\ 6.473 & -1.458 & 7.256 & 3.458 & 0 & 5.124 & 7.154 \\ 4.368 & -1.467 & 3.465 & 6.472 & 6.159 & 0 & 4.356 \\ 6.254 & -1.493 & 2.841 & 5.368 & 2.146 & 5.368 & 0 \end{bmatrix}$$

It can be seen from the fault judgment matrix that although not all elements in any one column are zero, all elements in the 2nd column of the matrix are not greater than 0, and all elements in the 2nd row are not less than 0. Therefore, it can be determined that the fault occurs on the branch M_2T_2 where M_2 is located. The distance from the fault point to the M_2 terminal can be calculated by formula (20).

$$dM_2 = 1.4 - 0.688 = 0.712km$$

Compared with the actual fault location at $0.7km$ from the M_3 terminal, the absolute error of the fault localization result is 12m. The localization accuracy results for faults occurring on other feeders are summarized in Table 3.

4.3 Line Faults Between Nodes

Simulate different types of faults at the line positions between different nodes in the multi-branch overhead line network. When an AB two-phase ground fault occurs at a position 3.5 km away from the M5 terminal on the line between node T_2 and node T_3 the fault judgment matrix

Table 3
Fault Localization Results for Branch Lines

Fault Location	Types of Faults	transition resistance /Ω	reference terminal	Fault Distance /km	Fault localization distance /km	fault localization error /m
M_1T_1	SLG	100	M_1	0.6	0.592	8
M_2T_2	3LG	600	M_2	0.7	0.712	12
M_3T_3	DLG	400	M_3	0.5	0.491	9
M_5T_5	OCF	1000	M_5	1.8	1.789	11
M_6T_6	LL	500	M_6	0.9	0.884	16
M_7T_4	SLG	800	M_7	1.2	1.190	10

Table 4
Location Results When a Fault Occurs on the Line between Two Nodes

Fault Location	Types of Faults	transition resistance /Ω	reference terminal	Fault Distance /km	Fault localization distance /km	fault localization error /m
T_1T_2	SLG	200	M_1	1.4	1.380	20
T_1T_4	OCF	1200	M_1	2.5	2.485	15
T_1T_6	3LG	800	M_6	1.3	1.291	9
T_3T_4	LL	600	M_3	1.6	1.582	18
T_4T_5	DLG	1000	M_5	3.5	3.514	14

obtained at this time is:

$$\delta' = \begin{bmatrix} 0 & 4.125 & 9.674 & 3.146 & 0 & 6.458 & 1.462 \\ 4.365 & 0 & 8.364 & 6.157 & 0 & 7.481 & 1.452 \\ 3.265 & 4.671 & 0 & 6.523 & 0 & 4.365 & 1.435 \\ 5.461 & 6.824 & 7.482 & 0 & 0 & 5.146 & 1.489 \\ 4.275 & 5.314 & 9.418 & 7.125 & 0 & 5.314 & 1.476 \\ 6.641 & 7.465 & 6.438 & 3.467 & 1.838 & 0 & 0 \\ 5.841 & 4.895 & 8.145 & 4.862 & 1.846 & 6.421 & 0 \end{bmatrix}$$

From the fault identification correction matrix, it can be observed that there is no column with all zero elements, indicating that the fault does not meet the conditions for a T-node fault. Meanwhile, there is also no column with all elements non-positive, implying that the branch M_iT_k fault condition is not satisfied either. However, the dot product of the elements in the 5th column and the 7th column equals zero, which allows the fault to be located on the line segment between the reference node T_4 at terminal M_7 and the reference node T_5 at terminal M_5. According to (20), the fault distance from terminal M_5 can be calculated as:

$$dM_5 = 2.7 + 0.814 = 3.514km$$

It can be observed that, compared to the actual fault location, which is $3.5km$ away from the M_5 terminal, the absolute error of the fault localization result is 14 meters. The localization accuracy results for faults occurring at other nodes are summarized in Table 4.

To verify the localization effect of the method proposed in this paper, different types of faults are set at different locations on the line and compared with the distribution network fault localization method proposed in Reference [22]. Table 5 presents the localization results of the method proposed in this paper, while Table 6 shows the localization results of the method in Reference [22]. The simulation results indicate that the localization accuracy of the method proposed in this paper is significantly improved compared with the method proposed in Reference [22], which enhances the fault localization performance by about 74.4% to 91.4% under different fault scenarios. When the fault occurs on the line between nodes,the localization error of the method proposed in this paper is lower than that of the method proposed in Reference [22], and it can accurately locate the fault point.

5. Conclusions

This paper proposes a fault localization method for multi-branch overhead distribution lines based on a cloud-edge collaborative architecture. By integrating the double-ended traveling wave ranging principle with a structural matrix construction approach, the method establishes a closed-loop collaborative framework for fault feature extraction, identification, and localization. A differential fault identification matrix combined with a correction margin mechanism is introduced to enhance the system's robustness against measurement deviations. Furthermore, a matrix feature matching strategy is employed to enable fast recognition and high-accuracy localization of various typical fault scenarios, including faults occurring at reference nodes, within branches, and between nodes. Simulation results demonstrate that the proposed method maintains a localization error within 20 meters across different fault types and locations. Compared with conventional

Table 5
The Fault Localization Results of the Method Proposed in this Paper

Fault Location	Types of Faults	transition resistance /Ω	reference terminal	Fault Distance /km	Fault localization distance /km	fault localization error /m
T_1T_4	SLG	200	M_1	3.5	3.516	16
M_4T_3	DLG	50	M_4	0.6	0.588	12
T_3T_4	3LG	400	M_3	1.8	1.845	15
M_7T_4	OCF	100	M_7	1.4	1.389	11
M_1T_4	LL	500	M_1	2.8	2.820	20

Table 6
The Fault Localization Results of the Method Proposed in Reference [22]

Fault Location	Types of Faults	transition resistance /Ω	reference terminal	Fault Distance /km	Fault localization distance /km	fault localization error /m
T_1T_4	SLG	200	M_1	3.5	3.686	186
M_4T_3	DLG	50	M_4	0.6	0.558	86
T_3T_4	3LG	400	M_3	1.8	1.926	126
M_7T_4	OCF	100	M_7	1.4	1.306	94
M_1T_4	LL	500	M_1	2.8	2.878	78

methods, the proposed approach achieves a substantial performance improvement, reducing the localization error by approximately 74.4% to 91.4% under various test scenarios. This indicates its strong engineering applicability, superior accuracy, and robust topological adaptability for complex distribution networks. To further improve the practical value of the approach, future work may incorporate optimization theory to develop an optimal deployment strategy for traveling wave acquisition devices, thereby minimizing resource allocation and maximizing efficiency while ensuring localization accuracy. This provides a feasible solution for fault diagnosis in large-scale distribution networks.

Funding Source:

Electric Power Research Institute of Guangxi Power Grid Co., Ltd.

Grant Numbers:

A Study on AC Test Energization and Fault Localization Techniques for Multi-Branch Overhead Distribution Lines (Grant No. GXKJXM20240123)

Conflicts of Interest:

None

Acknowledgment

This work was supported by the science and technology project of Guangxi Power Grid Co., Ltd., A Study on AC Test Energization and Fault Localization Techniques for Multi-Branch Overhead Distribution Lines, GXKJXM20240123.

References

[1] W. H. Guo, "Chain Fault Identification and Power Grid Planning Optimisation in Power Systems Considering Multiple Scenarios," *International Journal of Power and Energy Systems*, vol. 44, pp. 1–14, 2024.

[2] T. T. Zhang, S. H. Dai, and Z. X. Cai, "Planning and Fault Control of Urban Distribution Lines Through Optimal Design," *International Journal of Power and Energy Systems*, vol. 45, no. 1, pp. 19–25, 2025.

[3] M. Mohammadniaei, F. Namdari, M. R. Shakarami, and S. A. Mousavinick, "A Novel Single Sensor Based Fault/Branch Location Method in Distribution Systems Based on Combination of Game Theory and Dijkstra's Algorithm," *IET Generation, Transmission & Distribution*, vol. 6, no. 21, pp. 4433–4443, 2022.

[4] Y. Zhang, J. Wang, and M. E. Khodayar, "Graph-Based Faulted Line Identification Using Micro-PMU Data in Distribution Systems," *IEEE Transactions on Smart Grid*, vol. 11, no. 5, pp. 3982–3992, 2020.

[5] M. Caporuscio, A. Dupuis, and W. Löwe, "Data-Driven Ground-Fault Location Method in Distribution Power System with Distributed Generation," *arXiv preprint*, 2024.

[6] F. Conte, F. D'Agostino, B. Gabriele, G. P. Schiapparelli, and F. Silvestro, "Fault Detection and Localization in Active Distribution Networks Using Optimally Placed Phasor Measurement Units," *IEEE Transactions on Power Systems*, vol. 38, no. 1, pp. 714–727, 2022.

[7] S. Chandran, R. Gokaraju, and K. Narendra, "An Extended Impedance-Based Fault Location Algorithm in Power Distribution System with Distributed Generation Using Synchrophasors," *IET Generation, Transmission & Distribution*, vol. 18, no. 3, pp. 479–490, 2024.

[8] C. G. Arsoniadis and V. C. Nikolaidis, "Precise Fault Location in Active Distribution Systems Using Unsynchronized Source Measurements," *IEEE Systems Journal*, vol. 17, no. 3, pp. 4114–4125, 2023.

[9] R. Zhao, J. Lu, Q. Chen, N. Zhou, and H. Liu, "Application of a Centroid Frequency-Based Back Propagation Neural Network Fault Location Method for a Distribution Network Considering Renewable Energy Assessment," *Electronics*, vol. 13, no. 8, p. 1491, 2024.

[10] N. Sapountzoglou, J. Lago, and B. Raison, "Fault Diagnosis in Low Voltage Smart Distribution Grids Using Gradient Boosting Trees," *Electric Power Systems Research*, vol. 182, p. 106254, 2020.

[11] H. Mirshekali, R. Dashti, A. Keshavarz, and H. R. Shaker, "Machine Learning-Based Fault Location for Smart Distribution Networks Equipped with Micro-PMU," *Sensors*, vol. 22, no. 3, p. 945, 2022.

[12] G. Qiu, Z. Tang, and Z. Kuang, "A Local Fault Location Method of Distribution Network Based on Ant Colony Algorithm," in *2023 International Conference on Applied Intelligence and Sustainable Computing (ICAISC)*, (Dharwad, India), pp. 1–7, IEEE, 2023.

[13] B. L. Nguyen, T. V. Vu, T. T. Nguyen, M. Panwar, and R. Hovsapian, "Spatial-Temporal Recurrent Graph Neural Networks for Fault Diagnostics in Power Distribution Systems," *IEEE Access*, vol. 11, pp. 46039–46050, 2023.

[14] C. Haydaroğlu, H. Kılıç, B. Gümüş, and M. T. Özdemir, "Advancing Fault Detection in Distribution Networks with a Real-Time Approach Using Robust RVFLN," *Applied Sciences*, vol. 15, no. 4, p. 1908, 2025.

[15] Z. Zhou, Y. Wen, M. Deng, J. Ma, J. Zeng, and X. She, "Fault Location Method for New Distribution Networks Based on Waveform Matching of Time–Frequency Travelling Waves," *IET Smart Grid*, vol. 7, no. 6, pp. 929–939, 2024.

[16] P. O. K. Anane, Q. Huang, O. Bamisile, and P. N. Ayimbire, "Fault Location in Overhead Transmission Line: A Novel Non-Contact Measurement Approach for Traveling Wave-Based Scheme," *International Journal of Electrical Power & Energy Systems*, vol. 133, p. 107233, 2021.

[17] Y. Wang, T. Zheng, C. Yang, and L. Yu, "Traveling-Wave Based Fault Location for Phase-to-Ground Fault in Non-Effectively Earthed Distribution Networks," *Energies*, vol. 13, no. 19, p. 5028, 2020.

[18] J. W. Zhao, H. Hou, Y. Gao, Y. P. Huang, S. P. Gao, and J. N. Lou, "Single-Phase Ground Fault Location Method for Distribution Network Based on Traveling Wave Time-Frequency Characteristics," *Electric Power Systems Research*, vol. 186, p. 106401, 2020.

[19] X. Xu, F. Zhou, Y. Nie, W. Xu, K. Wang, J. OuYang, and Y. Han, "Fault Detection and Location of 35 kV Single-Ended Radial Distribution Network Based on Traveling Wave Detection Method," *Processes*, vol. 11, no. 8, p. 2494, 2023.

[20] C. Zhang, G. Song, L. Yang, and Z. Sun, "Time-Domain Single-Ended Fault Location Method That Does Not Need Remote-End System Information," *IET Generation, Transmission & Distribution*, vol. 14, no. 2, pp. 284–293, 2020.

[21] P. N. Ayambire, Q. Huang, A. K. Awopone, L. Jian, P. O. Anane, O. Bamisile, and Z. Zhang, "A Non-Contact Current Traveling Wave Fault Location Method for Multi-Terminal Overhead Power Lines Based on Adaptive Mathematical Morphology," *Electrical Engineering*, vol. 107, no. 1, pp. 191–204, 2025.

[22] J. Qiao, X. Yin, X. Liu, Y. Wang, and W. Xu, "An Accurate Fault-Location Method for Distribution Network with Distributed Generators Based on Multi-Terminal Traveling Wave," in *2020 IEEE Sustainable Power and Energy Conference (iSPEC)*, (Chengdu, China), pp. 1867–1873, IEEE, 2020.

[23] L. Cheng, T. Wang, and Y. Wang, "A Novel Fault Location Method for Distribution Networks with Distributed Generations Based on the Time Matrix of Traveling-Waves," *Protection and Control of Modern Power Systems*, vol. 7, no. 1, p. 46, 2022.

[24] I. Bzikha, P. Monferran, V. Velayudhan, and A. Reineix, "Analysis of Chaos Time Domain Reflectometry for the Soft Fault Detection in a Cable," in *2020 International Symposium on Electromagnetic Compatibility - EMC EUROPE*, (Rome, Italy), pp. 1–6, IEEE, 2020.

[25] W. Sima, H. Zhang, and M. Yang, "Edge–Cloud Collaboration Detection Approach for Small-Sample Imbalanced Faults in Power Lines," *IEEE Transactions on Instrumentation and Measurement*, vol. 71, pp. 1–11, 2022.

[26] F. Sanniti, S. D. Sessa, A. Greco, S. Talomo, M. Pajussin, and R. Benato, "TWMI: A Single-Ended Fault Location Method for Multi-Branch Earthed Overhead Lines Based on a Matrix Approach," in *2024 AEIT International Annual Conference (AEIT)*, (Trento, Italy), pp. 1–6, IEEE, 2024.

Biographies

Ziming Zhu received his Ph.D. degree in Electronic and Electrical Engineering from Loughborough University, United Kingdom, in 2014. Since then, he has been a senior engineer with the Electric Power Research Institute of Guangxi Power Grid Co., Ltd. His research interests include digital power grid, smart distribution network, and fault diagnosis.

Xiaoyong Yu received his M.S. degree in Control Theory and Control Engineering from Hohai University in 2010. Since then, he has been a senior engineer with the Electric Power Research Institute of Guangxi Power Grid Co., Ltd. His research interests include smart distribution networks and fault diagnosis.

Ke Zhou received his Ph.D. degree in Electrical and Information Engineering from Hunan University in 2007. Since then, he has been a senior engineer with the Electric Power Research Institute of Guangxi Power Grid Co., Ltd. His research interests include smart distribution networks, intelligent sensing and power chips, advanced power quality, and distribution network fault diagnosis.

Tanghua Wu received his Bachelor's degree from Xingjian College of Science and Liberal Arts, Guangxi University, in 2017. Since then, he has been a senior engineer with the Electric Power Research Institute of Guangxi Power Grid Co., Ltd. His research interests include distribution network operation and maintenance, distribution automation, and fault diagnosis in distribution networks.